Received: 9 September 2021 | Revised: 27 May 2022 | Accepted: 5 June 2022

DOI: 10.1111/acel.13660

Aging Cell WILEY

RESEARCH ARTICLE

DAF-2/insulin IGF-1 receptor regulates motility during aging by integrating opposite signaling from muscle and neuronal tissues

Charline Roy | Laurent Molin | Allan Alcolei | Mathilde Solyga | Benjamin Bonneau | Camille Vachon | Jean-Louis Bessereau | Florence Solari

Université de Lyon, Université Claude Bernard Lyon 1, CNRS UMR5284, INSERMU1314, Institut NeuroMyoGène, MeLis, Lyon, France

Correspondence
Florence Solari, Institut NeuroMyoGene, MeLis, 8 Av. Rockefeller, 69008 Lyon, France.
Email: florence.solari@univ-lyon1.fr

Present address
Benjamin Bonneau, Institut Curie, PSL Research University, Université Paris-Saclay, CNRS UMR3347, INSERM U1021, Orsay, France

Funding information
Agence Nationale de la Recherche, Grant/Award Number: ANR-11-LABX-0042; European Research Council, Grant/Award Number: ERC_Adg C.NAPSE #695295; Fondation de la recherche médicale (FRM), Grant/Award Number: FDT202106012780; Agence Nationale de la Recherche, Grant/Award Number: ANR-21-CE14-0026-01

Abstract

During aging, preservation of locomotion is generally considered an indicator of sustained good health, in elderlies and in animal models. In *Caenorhabditis elegans*, mutants of the insulin-IGF-1 receptor DAF2/IIRc represent a paradigm of healthy aging, as their increased lifespan is accompanied by a delay in age-related loss of motility. Here, we investigated the DAF-2/IIRc-dependent relationship between longevity and motility using an auxin-inducible degron to trigger tissue-specific degradation of endogenous DAF-2/IIRc. As previously reported, inactivation of DAF-2/IIRc in neurons or intestine was sufficient to extend the lifespan of worms, whereas depletion in epidermis, germline, or muscle was not. However, neither intestinal nor neuronal depletion of DAF-2/IIRc prevented the age-related loss of motility. In 1-day-old adults, DAF-2/IIRc depletion in neurons reduced motility in a DAF-16/FOXO dependent manner, while muscle depletion had no effect. By contrast, DAF-2 depletion in the muscle of middle-age animals improved their motility independently of DAF-16/FOXO but required UNC-120/SRF. Yet, neuronal or muscle DAF-2/IIRc depletion both preserved the mitochondria network in aging muscle. Overall, these results show that the motility pattern of *daf-2* mutants is determined by the sequential and opposing impact of neurons and muscle tissues and can be dissociated from the regulation of the lifespan. This work also provides the characterization of a versatile tool to analyze the tissue-specific contribution of insulin-like signaling in integrated phenotypes at the whole organism level.

KEYWORDS
DAF-16/FOXO, *daf-2*, insulin/IGF-1 signaling, lifespan, mitochondria, motility, oxidative stress, UNC-120/SRF

1 | INTRODUCTION

Aging has long been regarded as an inevitable process resulting from a gradual and passive deterioration over time, as illustrated by the "wear and tear" theory of aging. However, genetic studies in the nematode *Caenorhabditis elegans* have revealed that a single mutation in the *daf-2* gene can double lifespan (Kenyon et al., 1993). *daf-2* encodes the sole ortholog of the mammalian insulin and IGF-1 receptors (IIRc), and its role in regulating lifespan appears to be conserved in mammals (Kenyon, 2010). *daf-2* mutants were initially

isolated for their constitutive formation of diapausal larvae, called dauer (Daf-c phenotype). The long-lived and Daf-c phenotypes of *daf-2* mutants require the FOXO transcription factor DAF-16 (Ogg et al., 1997; Lin et al., 1997). Activation of the DAF-2/IIRc triggers a cascade of phosphorylation responsible for the retention of DAF-16/FOXO into the cytoplasm (Henderson & Johnson, 2001; Lee et al., 2001; Li et al., 2021; Lin et al., 2001). Down-regulation of this pathway promotes DAF-16/FOXO accumulation into the nucleus where it activates hundreds of genes (Tepper et al., 2013).

Decline in physical performance is a universal feature of aging. The motility phenotype of *daf-2* mutants has been controversial in the past, as they showed reduced motility in the presence of food and/or in the absence of stimulation due to a food-seeking defect (Churgin et al., 2017; Hahm et al., 2015; Hsu et al., 2009; Huang et al., 2004; Podshivalova et al., 2017). However, measurement of motility of *daf-2* mutant in the absence of food, either on plate or in liquid, has revealed that it is increased in middle-age compared to wild-type worms (Bansal et al., 2015; Hahm et al., 2015; Mulcahy et al., 2013). Thus, *daf-2* mutants are also considered to be healthier in later life, which may be due to preserved motoneurons function (Liu et al., 2013).

To date, very little is known about the physiological expression pattern of DAF-2/IIRc. An immunolabelling approach has shown that DAF-2/IIRc is expressed mainly in the nervous system and in a pair of cells called "XXX cells" in the head and also in the epidermis (Kimura et al., 2011). In addition, two studies analyzed the requirement of DAF-2/IIRc or DAF-16/FOXO in different tissues for lifespan regulation using transgene rescue of *daf-2* or *daf-2; daf-16* mutants (Libina et al., 2003; Wolkow et al., 2000). The first study concluded that DAF-2 acts primarily in the nervous system, consistent with the expression profile of DAF-2/IIRc, while DAF-16/FOXO was later shown to act principally in the gut. This was counter-intuitive because these two proteins function in the same signaling pathway. The paradox was resolved by proposing that intestinal DAF-16/FOXO may trigger a secondary signal from the gut to induce inhibition of DAF-2/IIRc in distant neuronal tissues (Libina et al., 2003). However, these studies were based on standard transgenic strategies, the only tools available at the time, which lack some of the regulatory elements present in the endogenous loci and also lead to the overexpression of proteins encoded by the transgenes. New technologies have been developed to manipulate the endogenous expression of specific proteins, providing a way to re-examine the tissue-specific activities of DAF2/IIRc, as we still do not know in which tissue wild-type DAF-2/IIRc functions for the regulation of the different phenotypes observed in *daf-2* mutants.

In this work, we investigated when and where DAF-2/IIRc is required to maintain worm motility during adulthood and how this phenotype relates to the dauer, lifespan and oxidative stress resistance phenotypes. In order to deplete DAF-2/IIRc protein in a spatially and temporally controlled manner, we generated alleles for conditional degradation by inserting an auxin-inducible degron (AID) (Zhang et al., 2015) and a fluorescent tag into the *daf-2* locus and constructed several independent strains to induce DAF-2/IIRc degradation in all cells or in neurons, muscle, intestine, germline or hypodermis. Previous studies used similar tools (Venz et al., 2021; Zhang et al., 2021) or tissue-specific CRISPR and RNAi approaches (Uno et al., 2021) to address the role of DAF-2/IIRc activity in the control of lifespan, dauer and oxidative stress resistance. Our work further explored the involvement of combinations of tissues in these phenotypes and more specifically investigated the regulation of motility, whose maintenance is commonly regarded as a characteristic of healthy aging.

Our results showed that DAF-2/IIRc is ubiquitously expressed in worms and can be efficiently degraded by the AID system. Degradation of DAF-2/IIRc in all tissues, from adulthood onwards, reproduced the lifespan and motility phenotypes of the reference *daf-2(e1370)* allele and the constitutive dauer phenotype in the progeny. Depletion of DAF-2/IIRc in neurons or in the gut was sufficient to extend the lifespan of the worms and only intestinal inactivation of DAF-2/IIRc reproducibly increased resistance to oxidative stress. Still, neither neuronal nor intestinal inactivation improved worm motility in adulthood. Neuronal depletion of DAF-2/IIRc unexpectedly downregulated motility from early adulthood, in a DAF-16/FOXO dependent manner. In contrast, muscle depletion was sufficient to improve motility in middle-aged worms, without affecting lifespan or resistance to oxidative stress. Finally, muscle inactivation of DAF-2/IIRc induced nuclear accumulation of DAF-16/FOXO in cells but did not require its activity for the regulation of motility which relies on the transcription factor UNC-120/SRF.

2 | RESULTS

2.1 | The AID::mNeonGreen-tagged DAF-2 protein is functional and efficiently downregulated in the presence of auxin

The mNeonGreen (mNG) and degron sequences were added to the 3′ end (before the STOP codon) of the endogenous *daf-2* locus (*daf-2::AID::mNG or kr462*) so that DAF-2 degradation could be monitored via the loss of mNG fluorescence. DAF-2::AID::mNG was detected in head neurons, XXX cells and epidermis as reported earlier (Kimura et al., 2011) but also in the majority of the worm tissues, from the two-cell stage embryo (Figure 1a). *daf-2(kr462)* worms were crossed with two independent lines that expressed in all tissues the plant ubiquitin ligase substrate recognition subunit, TIR1, an essential component of the AID system (see Table S1 for strain description). We then verified that neither the tag nor the presence of the TIR1 transgene interfered with DAF-2 function. In the absence of auxin, *daf-2(kr462)* and *daf-2(kr462)*; *Pubiquitous::TIR1* worms exhibited the same lifespan (Figure 1b,c; Table S2) and motility (Figure 1d,e) as wild-type worms. Furthermore, they did not enter the dauer stage at any temperature in the presence of food (Table S3), in contrast to the heat-sensitive reference *daf-2(e1370)* mutants that showed a fully penetrant dauer constitutive phenotype. Thus, the addition of the degron and mNG sequences to the

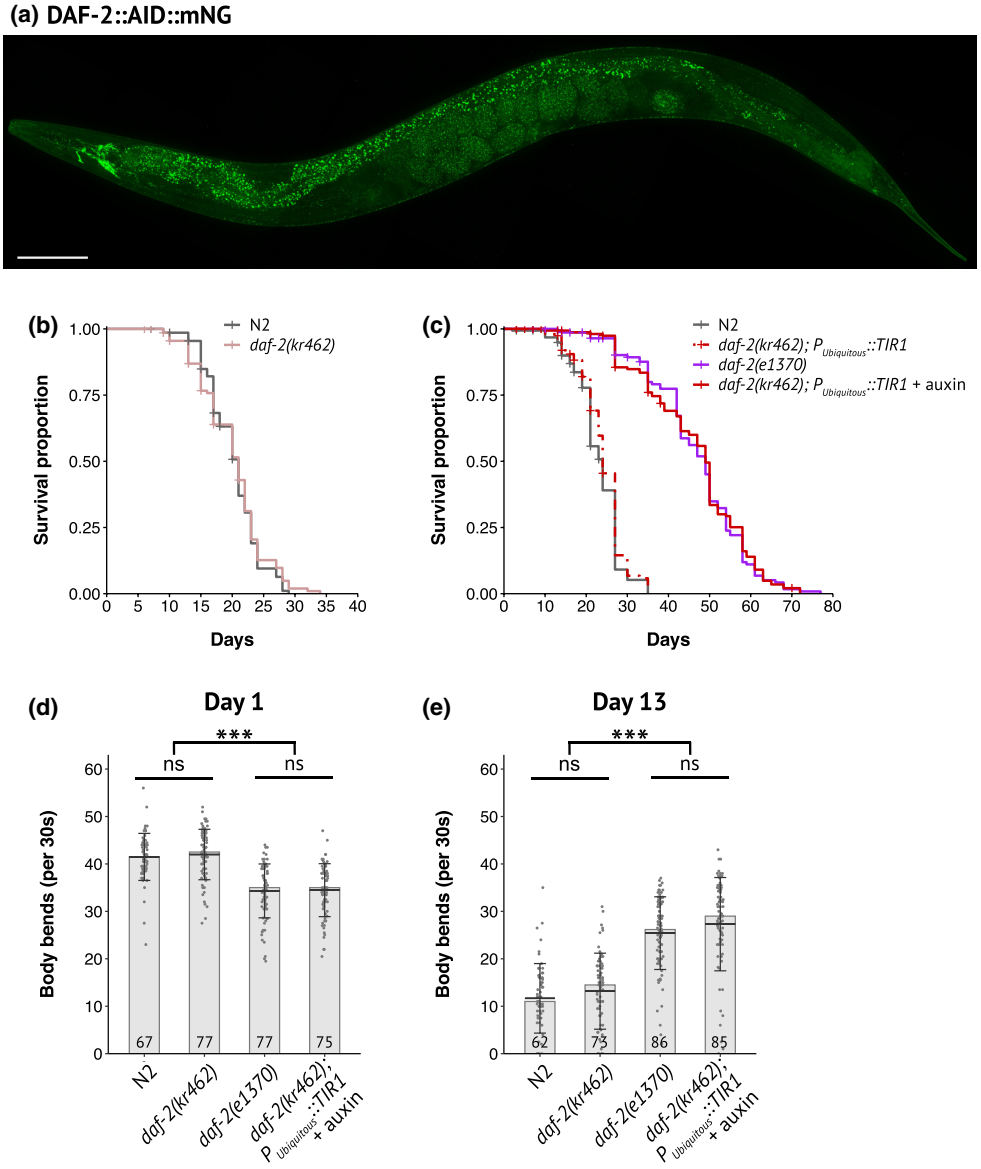

FIGURE 1 Expression pattern of DAF-2::AID::mNG and functional validation of its degradation by the auxin-inducible system. (a) Image of DAF-2::AID::mNG in 1-day-old *daf-2(kr462)* adult. Scale bar: 100 µm. (b) Survival curves of control (N2) and *daf-2(kr462)* animals ($N = 2$, $n = 141$ and 138 for N2 and *daf-2(kr462)*, respectively). (c) Survival curves of N2, *daf-2(e1370)* mutants, and worms with ubiquitous depletion of DAF-2. Data have been pooled from two independent experiments ($n = 155–160$ for each genotype) in which two different *Peft-3::TIR1* containing strains were tested. See Table S1 for strain description and Table S2 for detailed lifespan data, replicates, and statistics. (d, e) Body bends frequency at day 1 (d) and day 13 (e) of adulthood of N2, *daf-2(e1370)*, or *daf-2(kr462)* worms, with or without ubiquitous expression of TIR1. The number of animals scored is indicated in each bar and corresponds to the pool of two experiments (see Figure 4 for more replicates). Bars indicate median values, means are represented by black horizontal lines, and brackets show standard deviations, ns: non-significant, ***: $p < 0.001$, Kruskal–Wallis and Dunn's post hoc test with FDR method for adjusting p-value. All experiments were performed at 20°C

daf-2 locus or TIR1 ubiquitous expression did not seem to impair DAF-2 function.

In the presence of auxin, the fluorescence signal was strongly downregulated, confirming the efficiency of auxin-induced DAF-2 degradation (Figure 2 and Figure S1a). We then assessed the dauer, lifespan and motility phenotypes of *daf-2(kr462)* worms expressing TIR1 in all tissues compared to *daf-2(e1370)* mutants. All transgenic worms placed on auxin from hatching entered the dauer stage at 15, 20 or 25°C, (Table S3 and Venz et al., 2021) mimicking the fully penetrant dauer phenotype of *daf-2(e1370)* mutants raised at the restrictive temperature of 25°C. Furthermore, when *daf-2(kr462)* worms were placed on auxin plates at a later developmental stage (L4) to bypass the dauer arrest, their lifespan was doubled, as *daf-2(e1370)* worms at 20°C (Figure 1c and Table S2). Remarkably, the ubiquitous degradation of DAF-2 also recapitulated the age-dependent motility phenotype of *daf-2(e1370)* mutants. Indeed, 1-day-old and 13-day-old *daf-2(kr462)* worms expressing TIR1 in all tissues showed a lower and higher frequency of body bends,

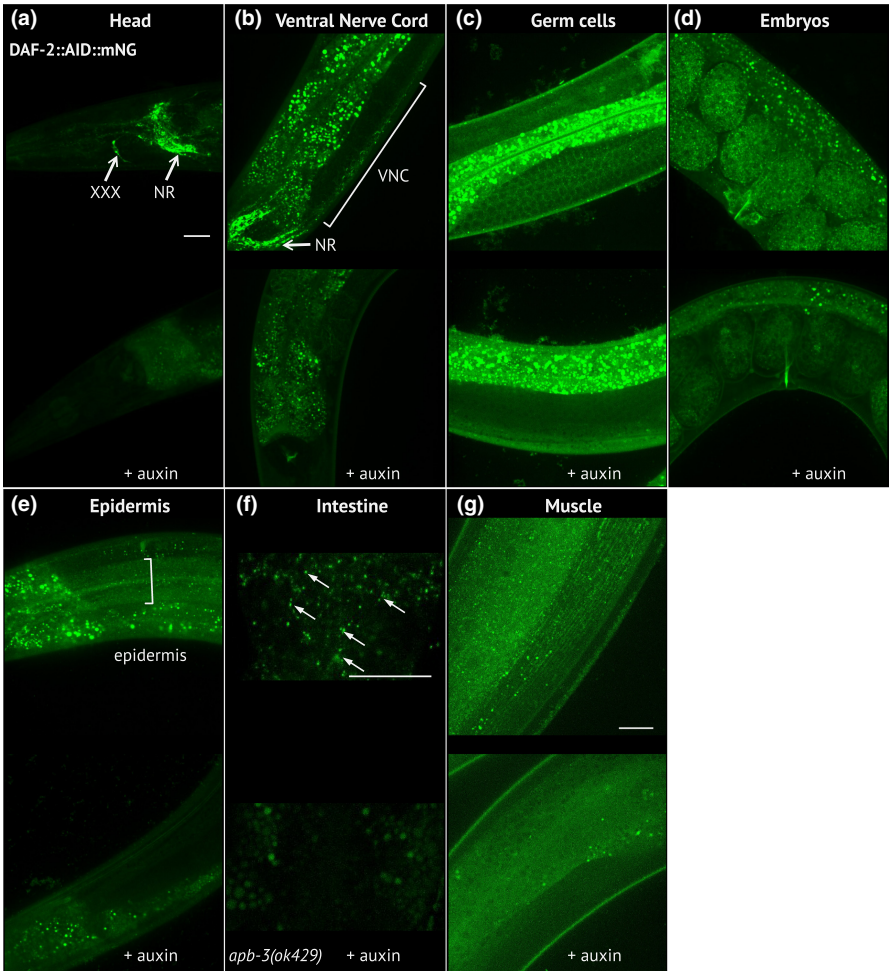

FIGURE 2 DAF-2::AID::mNG is effectively downregulated in the presence of ubiquitously expressed TIR1 after auxin treatment. (a–g) Images of DAF-2::AID::mNG in 1-day-old *daf-2(kr462)* adults expressing ubiquitous TIR1 and grown in the absence of auxin (upper panels) or after 24 h of auxin treatment (lower panels). Images focus on specific body regions: the head (a), showing strong expression in the nerve ring (NR) and the XXX cells; the neuronal cell bodies of the ventral nerve cord (VNC) (b); the proliferating germ cells (c); the embryos (d); the epidermal syncytium (e); the intestine (f) and the body wall muscles (g). For the intestine (f), images were taken in *apb-3(ok429)* mutant background in order to reduce unspecific intestinal autofluorescence (arrows indicate the specific DAF-2::AID::mNG associated signal). In all images, the remaining staining of the gut after auxin treatment corresponds to nonspecific autofluorescence that varies between animals. Similar results were obtained in 7-day-old animals (data not shown). Scale bars: 20 μm

respectively, compared to control animals of the same age (Figure 1d,e). Overall, these data demonstrate that the downregulation of DAF-2::AID::mNG correlates with a significant reduction of DAF-2 function, validating our experimental approach. However, the reference *daf-2(e1370)* allele is considered hypomorphic because predicted null *daf-2* mutations cause early developmental phenotypes with embryonic arrest (Gems et al., 1998). This suggests that some DAF-2 protein persists, consistent with the low level of fluorescence still detected in the presence of auxin (Figure 2). Nevertheless, our results show that inactivation of DAF-2 during development is not a prerequisite for lifespan extension, in agreement with previous results (Dillin et al., 2002; Venz et al., 2021) and that down-regulation of DAF-2 in adulthood is also sufficient to recapitulate the effect of constitutive down-regulation of DAF-2 on worm motility during aging.

2.2 | Intestinal and neuronal DAF-2 activities cooperate to regulate lifespan but are differently required for the resistance of worms to oxidative stress

We first examined the tissue-specific contribution of DAF-2 inactivation to the regulation of dauer and lifespan. Transgenic lines were generated to express TIR1 in muscle (*Pmyo-3*), hypodermis (*Pdpy-17*), neurons (*Prab-3*), gut (*Pges-1*), or germline (*Psun-1*). In addition to the previously described TIR1 transgenes, we generated new transgenes in order to test two independent lines for each tissue and thus limit potential confounding effect of the genetic background (see Experimental procedures and Table S1). In the presence of auxin, these TIR1 transgenes allowed efficient degradation of the DAF-2::AID::mNG protein in individual tissues, as indicated

by the loss of fluorescent signals in young and middle-aged adults after 24 h (Figure S1b–h) and by DAF-16 nuclear accumulation (see below, result Section 4). Dauer formation could not be achieved after degradation of DAF-2 in one given tissue (Table S3) thus suggesting that DAF-2 functions in several tissues and/or in cells other than the main tissues tested to control dauer entry, as also shown by Venz et al. (2021). These observations are in contradiction with previous data showing that overexpression of *daf-16* in the nervous system of *daf16; daf-2* double mutants recapitulated the Daf-c phenotype of *daf-2* mutants (Libina et al., 2003). However, recent work on the tissue-specific activities of DAF-16 in a wild-type context argues that DAF-16 is required in several tissues to control the dauer phenotype (Aghayeva et al., 2021), in agreement with our results with DAF-2.

Inactivation of DAF-2 in muscle, hypodermis, or germline did not reproducibly affect lifespan suggesting that depletion of DAF-2 in these tissues may not be sufficient to impact this phenotype (Figure 3a–f; Figure S2d–g and Table S2). However, we cannot completely rule out that a small amount of undegraded DAF-2 remained in these tissues.

Degradation of DAF-2 in neurons or intestine was sufficient to increase the mean lifespan by 37% and 53%, respectively. However, none of these tissues recapitulated the lifespan increase caused by ubiquitous DAF-2 inactivation (Figure 3g–j; Figure S2h, i). Combined DAF-2 degradation in both neurons and gut did not further extend the lifespan of animals as compared to worms with intestinal or neuronal DAF-2 degradation alone (Figure 3k; Figure S2j). Thus, additional cells or a different combination of tissues may be involved in the regulation of lifespan by DAF-2.

Resistance to oxidative stress has been proposed as a mechanism responsible for the extension of lifespan by DAF-2 (Honda & Honda, 2002). In the presence of 20 mM paraquat, a reactive oxygen species generator, ubiquitous or intestinal inactivation of DAF-2 consistently increased the survival of worms compared to control worms, although to a lesser extent for intestinal lines (Figure 3L; Figure S2k,l,n). Neuronal inactivation of DAF-2 reproducibly resulted in a slight increase in paraquat resistance in one line, and a slightly lower resistance in the second (Figure 3m, Figure S2l,m,n), although both lines were long-lived in the absence of paraquat (Figure 3i,j). In addition, neuronal inactivation of DAF-2 reduced the resistance to oxidative stress of worms with intestinal DAF-2 depletion (Figure 3n, Figure S2n), but did not shorten their lifespan (Figure 3k). These data suggest that neuronal and intestinal inactivation of DAF-2 triggers lifespan extension mechanisms that are at least partially independent of oxidative stress resistance.

2.3 | DAF-2 neuronal signaling is required for worm motility in early adulthood, while DAF-2 muscle signaling impairs motility from mid-adulthood

In order to further characterize the fitness of long-lived worms, we measured their body-bend frequency in liquid medium (BBF), as a proxy of physical performance (Duhon & Johnson, 1995; Laranjeiro et al., 2019). The motility of worms with DAF-2 inactivation in the intestine was similar to that of control worms on days 1 and 13 of adulthood (Figure 4a–c). Thus, the signaling from the intestine upon DAF-2 degradation is sufficient to prolong lifespan, but does not markedly affect the function of the neuromuscular system with age.

Neuronal inactivation of DAF-2 significantly reduced the worm's BBF of 1-day-old animals and mirrored the motility phenotype of animals with whole-body degradation of DAF-2 (Figure 4a). This reduction was unexpected as Liu et al. reported an increased neurotransmission at the neuromuscular junction (NMJ) of *daf-2(e1370)* mutants, although for later age (Liu et al., 2013). We thus assessed cholinergic neurotransmission in our strains by treating worms with aldicarb. Aldicarb is an inhibitor of acetylcholinesterase, which induces worm paralysis due to the accumulation of acetylcholine in the synaptic cleft. Consistent with Liu et al. data, we observed an increase in cholinergic neurotransmission, indicated by an accelerated paralysis in response to aldicarb, when DAF-2 was ubiquitously inactivated in middle-aged animals but also in 1-day-old animals (Figure S3). However, worms with neuronal depletion of DAF-2 behaved on aldicarb like control worms (Figure S3).

The regulation of worm motility relies on a complex neuronal network that involves different class of interneurons, excitatory cholinergic and inhibitory GABAergic motoneurons (Zhen & Samuel, 2015). Previous report showed that DAF-2 is expressed in both cholinergic and GABAergic neurons (Taylor et al., 2021). Depletion of DAF-2 in either cholinergic or GABAergic neurons only was sufficient to impede worm's motility in 1-day-old animals, thus suggesting that DAF-2 functions in both types of neurons to control motility in young adults (Figure 4b).

In contrast to neuronal DAF-2, muscle inactivation of DAF-2 did not affect the BBF of 1-day-old adult animals but was sufficient to recapitulate the higher BBF of 13-day-old adult animals with ubiquitous DAF-2 depletion (Figure 4a,c), although it affected neither lifespan (Figure 3a,b; Figure S2d) nor resistance to oxidative stress (Figure S2o,p). Furthermore, inactivation of DAF-2 in neurons did not suppress the beneficial impact of muscle DAF-2 inactivation on motility (Figure 4c).

Taken together, these data support a critical role for wild-type DAF-2 activity in muscle in negatively regulating motility in middle age, while neuronal DAF-2 promotes motility in early adulthood.

2.4 | DAF-16 nuclear accumulation upon tissue-specific inactivation of DAF-2

Early studies on the tissue-specific activities of DAF-2 and DAF-16 have suggested that down-regulation of the DAF-2 signaling pathway in one tissue induces its inhibition in distant tissues (Libina et al., 2003; Wolkow et al., 2000). However, these results were obtained in a sensitized genetic background, as all cells were mutant for *daf-2*. More recent data supported this model in a *daf-2(+)* background by showing that overexpression of intestinal or neuronal DAF-16 induces nuclear

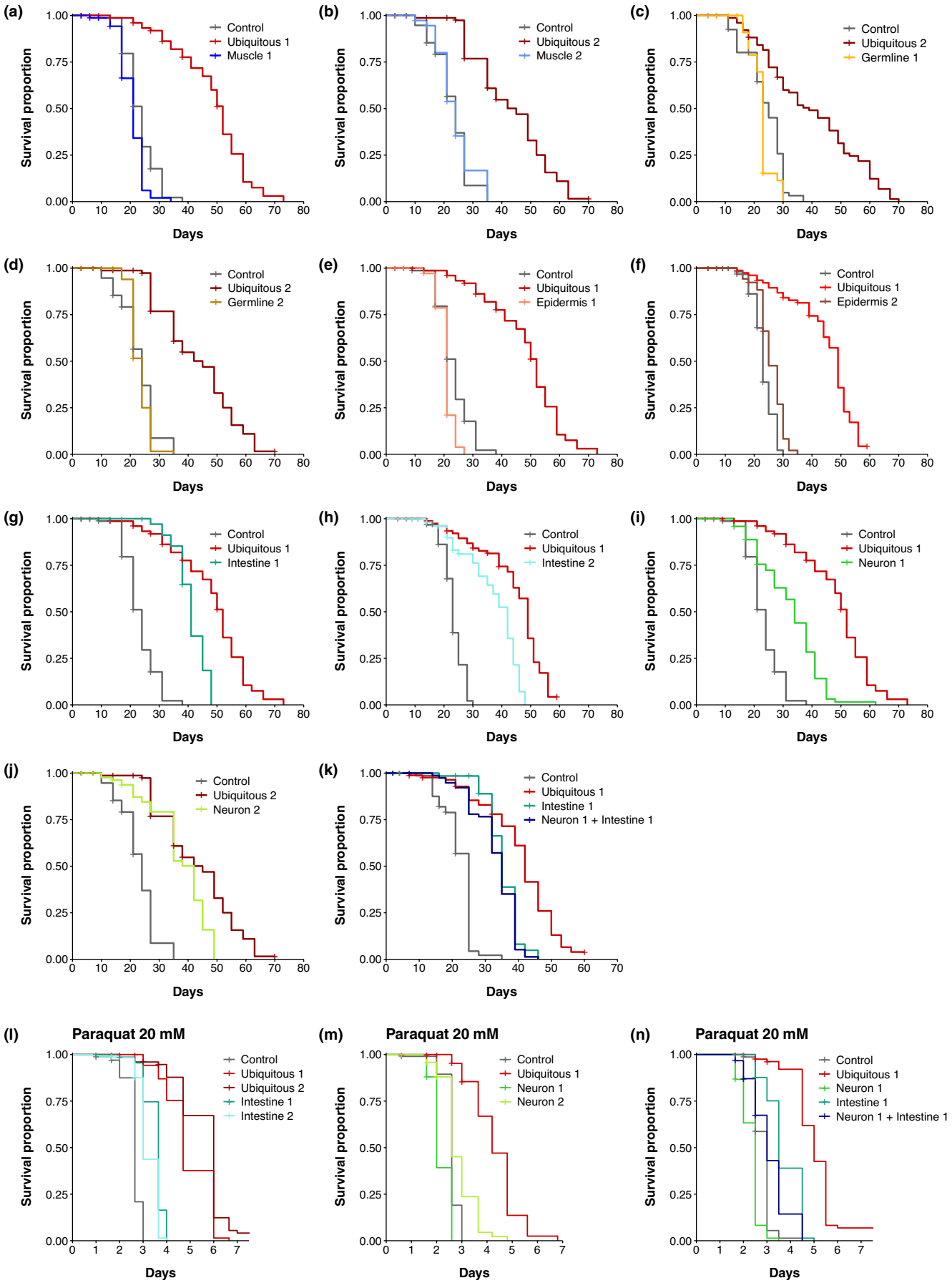
(a)
Control
Ubiquitous 1
Muscle 1
(b)
Control
Ubiquitous 2
Muscle 2
(c)
Control
Ubiquitous 2
Germline 1
(d)
Control
Ubiquitous 2
Germline 2
(e)
Control
Ubiquitous 1
Epidermis 1
(f)
Control
Ubiquitous 1
Epidermis 2
(g)
Control
Ubiquitous 1
Intestine 1
(h)
Control
Ubiquitous 1
Intestine 2
(i)
Control
Ubiquitous 1
Neuron 1
(j)
Control
Ubiquitous 2
Neuron 2
(k)
Control
Ubiquitous 1
Intestine 1
Neuron 1 + Intestine 1
(l)
Paraquat 20 mM
Control
Ubiquitous 1
Ubiquitous 2
Intestine 1
Intestine 2
(m)
Paraquat 20 mM
Control
Ubiquitous 1
Neuron 1
Neuron 2
(n)
Paraquat 20 mM
Control
Ubiquitous 1
Neuron 1
Intestine 1
Neuron 1 + Intestine 1
Survival proportion
Days

FIGURE 3 Inactivation of DAF-2 in neurons or in the gut is sufficient to increase lifespan. (a–k) Survival curves of animals with DAF-2 depletion in all cells (a–k), muscle (a, b), germline (c, d), epidermis (e, f), intestine (g, h), neurons (i, j), or neurons and intestine (k). Numbers (e.g. Muscle 1, Muscle 2) refer to distinct alleles driving TIR1 expression (see Table S1). For each condition, n is about 80 individuals. Some experiments were split in separate graphs for clarity; thus, some graphs share the same negative and positive controls: (a), (e), (g), (i); (b), (d), (j); (f) and (h). The control conditions correspond to the N2 or *daf-2(kr462)* strains, in the presence of EtOH or auxin, whose lifespans did not show significant differences. (l–n) Survival curves of animals with DAF-2 depletion in all cells (l–n), intestine (l), neurons (m), or neurons and intestine (n) in presence of 20 mM paraquat. Controls correspond to *daf-2(kr462)*. All strains have been treated with auxin. For each condition, 75 to 100 individuals have been assayed. For detailed lifespan data, replicates, statistics, and summary of independent assays see Table S2 and Figure S2

accumulation of DAF-16::GFP in distant tissues (Uno et al., 2021). To avoid potential issues associated with reporter transgenes such as overexpression, we endogenously tagged DAF-16/FOXO with wrmSCARLET using CRISPR/Cas9 mediated genome engineering. DAF-16::wrmSCARLET was detected in all somatic tissues and the germline during adulthood, with highest expression in neurons, and localized mainly in the cytoplasm of all cells (Figure 5a and Table S4). Ubiquitous depletion of DAF-2 from the L4 stage induced nuclear accumulation of DAF-16 in all tissues (Figure 5b) and the whole progeny entered the dauer stage (data not shown), confirming that the DAF-16::wrmSCARLET protein was functional.

Depletion of DAF-2 in the intestine was associated with nuclear accumulation of DAF-16::wrmSCARLET in the gut and distant tissues that do not seem to include neurons (Figure 5c). In contrast, tissue-specific degradation of DAF-2 in neurons or muscle from L4 onwards induced nuclear accumulation of DAF-16::wrmSCARLET in the same tissue but not in distant tissues (Figure 5d,e). This suggests that the regulation of motility by neuronal and muscle DAF-2 activity does not rely on DAF-2 inactivation in distant tissues.

2.5 | The control of motility by the neuronal and muscle activities of DAF-2 requires DAF-16 and UNC-120, respectively

To investigate the functional significance of cell-autonomous regulation of DAF-16 nuclear accumulation by DAF-2, we crossed worms in which DAF-2 is inactivated in muscle or neuronal cells with worms carrying the *daf-16(ot853)* allele that encodes DAF-16::mNeonGreen::AID (Bhattacharya et al., 2019). *daf-16(ot853); daf-2(kr462)* worms showed a slight reduction in motility compared to control *daf-2(kr462)* worms (Figure 6a). Nevertheless, neuronal degradation of DAF-16 improved the motility of worms with neuronal inactivation of DAF-2 (Figure 6a). These data strongly suggest that inactivation of DAF-16 suppressed the motility phenotype associated with DAF-2 neuronal depletion. In contrast, the increase in motility of 13-day-old animals with muscle inactivation of DAF-2 was not affected by depletion of DAF-16 in the same tissue (Figure 6b). We then tested whether the transcription factor UNC-120/SRF was required, as we have previously shown that inhibition of *unc-120* expression in *daf-2(e1370)* mutants significantly reduced their motility from mid-adulthood (Mergoud Dit Lamarche et al., 2018). Furthermore, *unc-120* is expressed in muscles, but not in neurons (Mergoud Dit Lamarche et al., 2018). RNAi mediated inactivation of *unc-120* from adulthood in worms with muscle-specific inactivation of DAF-2 also suppressed DAF-2 impact on worm motility (Figure 6c).

Overall, while DAF-16 accumulated in the nuclei of neurons or muscles after inactivation of DAF-2 in the same tissue, it is essential for the regulation of motility in neurons but not in muscles in which DA-F2 required UNC-120 for motility regulation.

2.6 | Both neuronal and muscular DAF-2 depletion prevents muscle mitochondria fragmentation with age

We and others (Mergoud Dit Lamarche et al., 2018; Regmi et al., 2014; Sharma et al., 2019) have previously shown that the morphology of muscle mitochondria changes from an interconnected to a fragmented network during muscle aging and that this phenotype is associated with loss of motility in old age. To further investigate the cell-autonomous function of DAF-2 in muscle aging, we monitored the muscle mitochondria pattern with age. We visualized mitochondria by expressing a single-copy insertion of a reporter encoding the N-terminal segment of TOMM20 (responsible for its anchoring to the mitochondrial outer membrane) fused to the fluorescent protein wrmSCARLET, under the control of the muscle *Pmyo-3* promoter (see Experimental procedures). It is noticeable that previously characterized worm strains carrying similar reporters but as an integrated multicopy array showed earlier mitochondrial fragmentation, probably due to overexpression of the fusion protein (Mergoud Dit Lamarche et al., 2018; Regmi et al., 2014). The ubiquitous degradation of DAF-2 delayed the fragmentation of mitochondria (Figure S4) in agreement with previous observations with the *daf-2(e1370)* mutant (Mergoud Dit Lamarche et al., 2018). Muscle inactivation of DAF-2 was sufficient to prevent muscle mitochondria fragmentation. However, neuronal depletion of DAF-2 gave similar results, alone or in combination with muscle depletion of DAF-2 (Figure S4). Thus, inactivation of DAF-2 in muscles or neurons is sufficient to prevent muscle mitochondrial fragmentation, suggesting that DAF-2 acts both autonomously and non-autonomously to maintain muscle integrity during aging.

3 | DISCUSSION

In this work, we investigated the relationship between lifespan and motility phenotypes caused by DAF-2/IIRc inactivation by analyzing

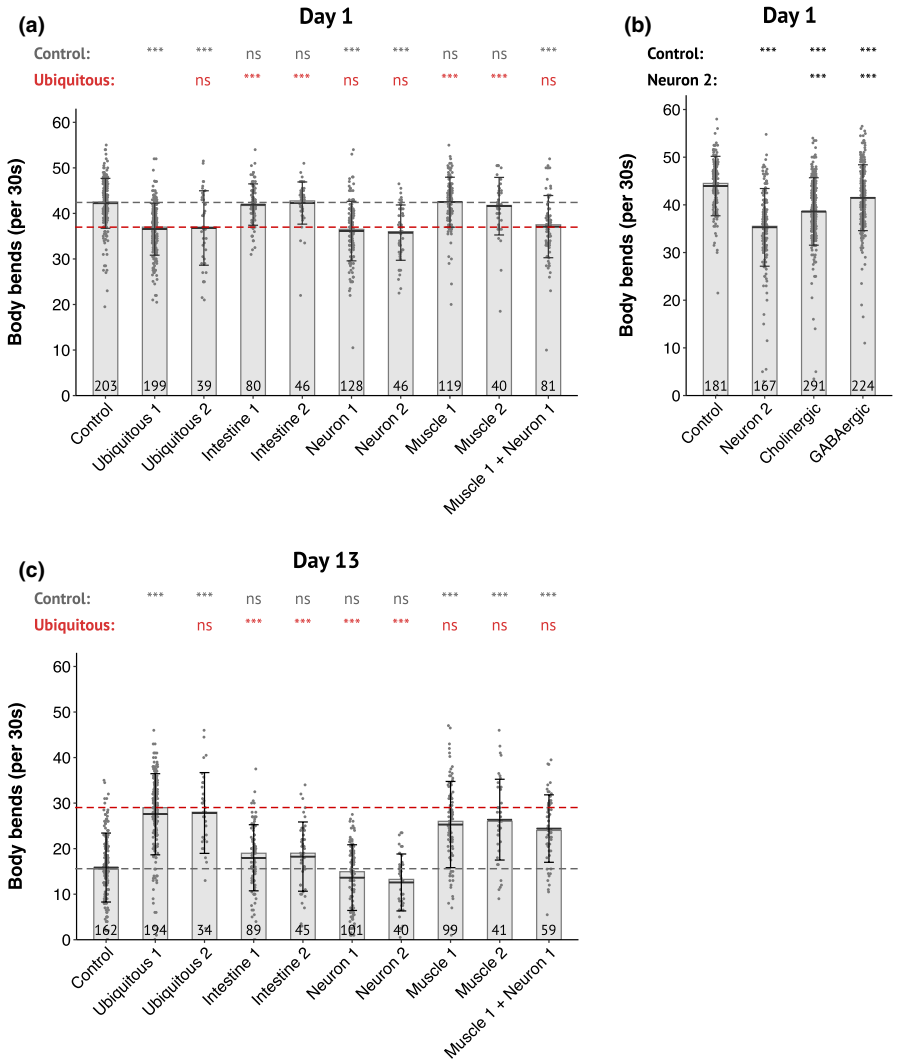

FIGURE 4 DAF-2 degradation in neurons or muscles differentially alters motility in an age-dependent manner. (a–c) Body bends frequency of 1-day-old (a, b) and 13-day-old (c) adults with depletion of DAF-2 in all cells or in the intestine, muscle, neurons or muscle and neurons as indicated. Control corresponds to *daf-2(kr462)* in presence of auxin. Numbers (e.g., Muscle 1, Muscle 2) refer to distinct alleles driving TIR1 expression (see Table S1). (a and c) Pooled data from 5 independent experiments. Each replicate included the control strain and several tissue-specific strains. (b) Pooled data from 7 independent experiments in which were assayed 4 and 3 independent lines for depletion of DAF-2 in cholinergic or GABAergic neurons, respectively. The number of animals scored is indicated in each bar. The bars correspond to the median values, the means are represented by black horizontal lines, and brackets show standard deviations. The dotted lines correspond to the median values for the control (gray) and ubiquitous (red) strains. Comparisons were done with Kruskal–Wallis, Dunn post hoc tests with FDR method to adjust *p*-value, ns: not significant, ***: $p_{adjusted}$ <0.001. Statistics are presented as two lines that include comparison with the control strain or with one specific strain (ubiquitous 1 for (a and c) and neuron 2 for (b))

the tissue-specific functions of DAF-2/IIRc in the regulation of these phenotypes. To this end, we have created a reporter line that allows the visualization of both DAF-2/IIRc expression and its degradation by the TIR1 auxin-inducible system in live animals.

3.1 | *daf-2(kr462)* transgenic animals as a model to study DAF-2 expression and function

As in other species, multiple isoforms of DAF-2/IIRc have been described, including DAF-2A and DAF-2C, which differ by the size of the α-chain of the α2β2 tetramer, and are analogous to mammalian IR-A and IR-B, respectively (Ohno et al., 2014). The mNeonGreen tag was inserted into the C-terminus shared by these two isoforms which control lifespan, dauer, heat tolerance (A and C) and avoidance behavior (C only). Three shorter isoforms have been reported (Ohno et al., 2014). DAF-2B, which retains the extracellular ligand-binding domain but lacks the intracellular signaling domain, modulates insulin signaling by sequestering insulin peptides, but its expression is restricted to the developmental larval stages and is no longer observed in the adult stage (Martinez et al., 2020). The DAF-2D and E isoforms lack part of the β-chain and the IRS1

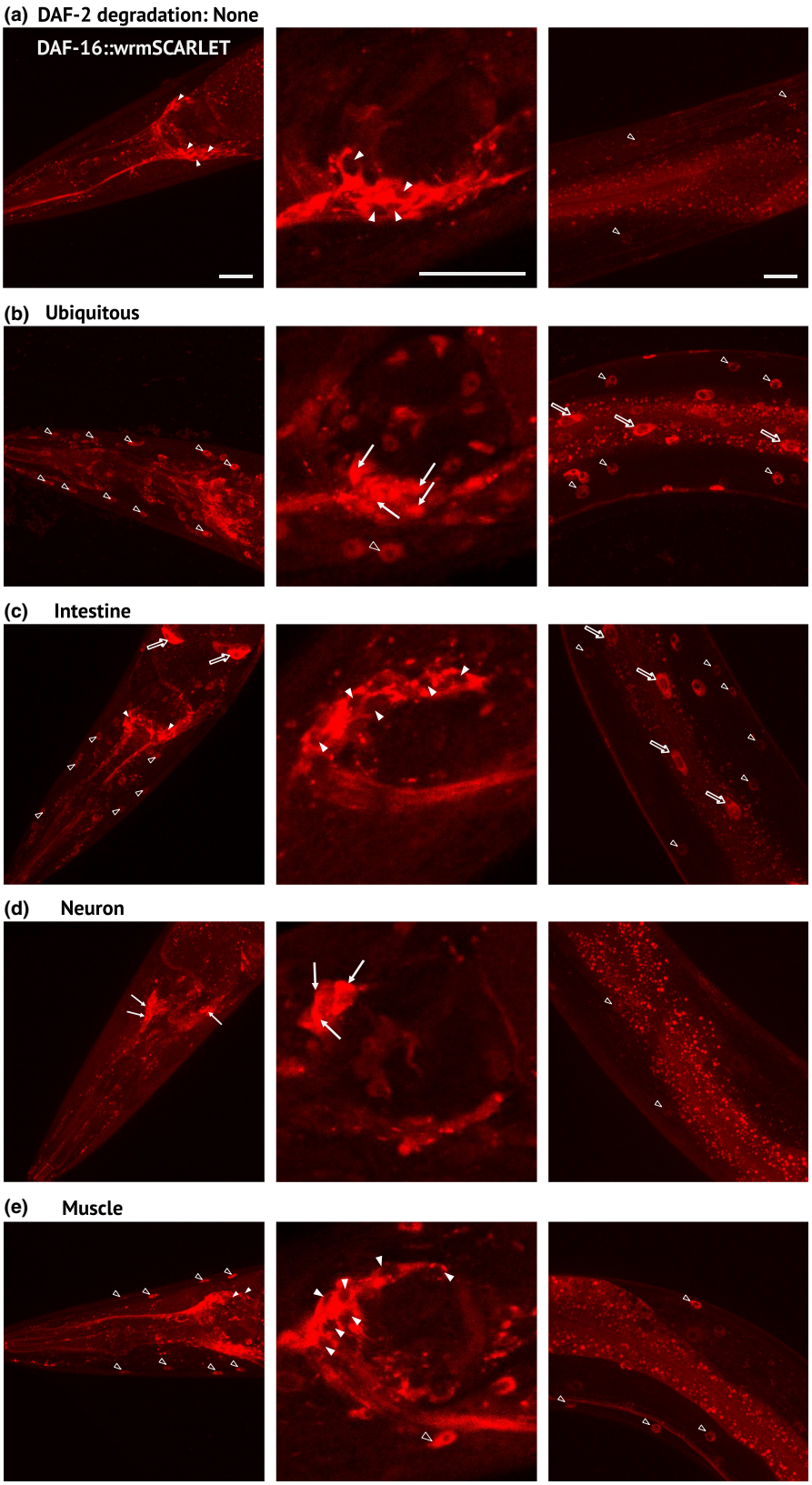

FIGURE 5 Regulation of DAF-16 subcellular localization by tissue-specific depletion of DAF-2 (a-e) Images of DAF-16::wrmSCARLET in the head (left and middle panels) or the anterior body (right panels) of 1-day-old *daf-16(kr535); daf-2(kr462)* adults without (a) or with ubiquitous (b), intestinal (c), neuronal (d) or muscular (e) depletion of DAF-2 caused by 24 h of auxin treatment (b–e). Empty arrowheads, full arrows and empty arrows indicate muscle, neuron and intestinal nuclei, respectively; full arrowheads correspond to the cytosol of neurons. For numbers and percentage of worms with a strong DAF-16::wrmSCARLET nuclear signal, see Table S4. Scale bars: 20 μm

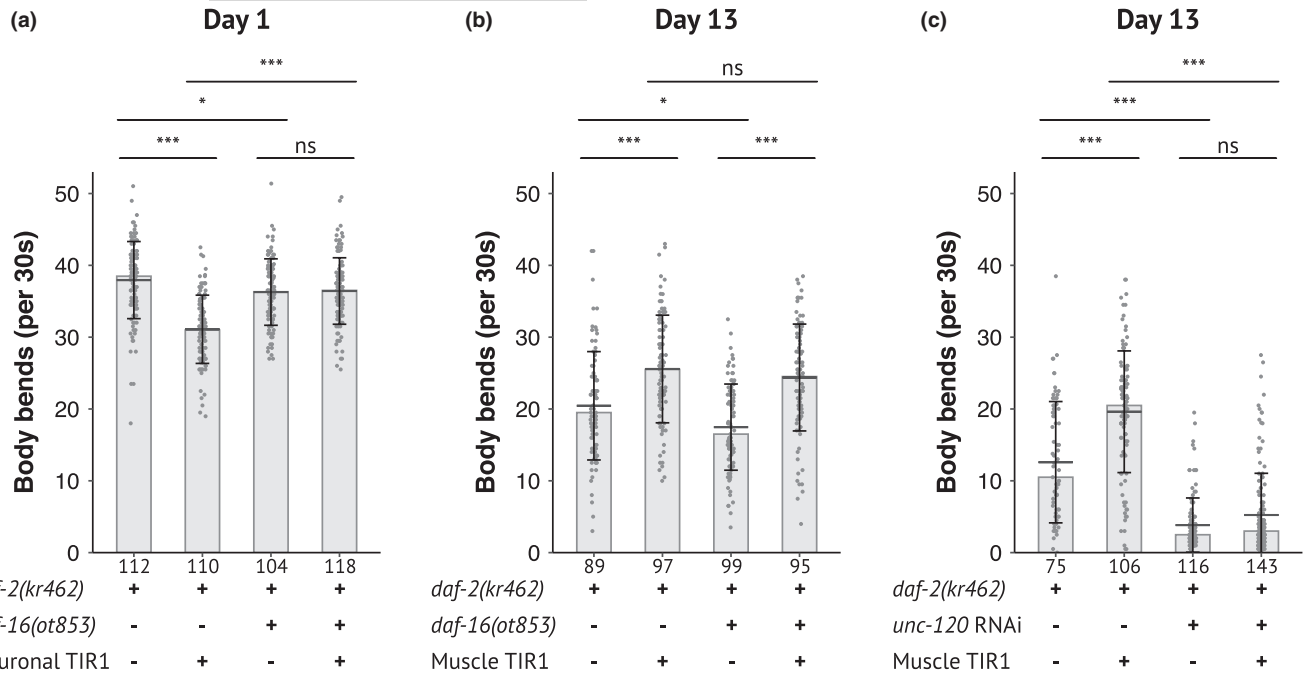

FIGURE 6 DAF-16 is required for motility regulation when DAF-2 is inactivated in neurons but not in muscles. Body bends frequency of 1-day-old (a) and 13-day-old (b, c) adults with depletion of DAF-2 and DAF-16 in neurons or muscle (a, b) or with down-regulation of *unc-120* by RNAi in a *rrf-3(pk1426)* genetic background (c) (see Experimental procedure and Table S1 for detailed genotype of strains). Data from three independent experiments were pooled. The number of animals scored is indicated under each bar. The bars correspond to the median values, the means are represented by black horizontal lines, and brackets show standard deviations. Comparisons were done with Kruskal–Wallis, Dunn post hoc tests with FDR method to adjust *p*-value, ns: not significant, *: $p_{adjusted}$ <0.05, ***: $p_{adjusted}$ <0.001

interaction domain, and their function remains to be defined. We showed that ubiquitous inactivation of DAF-2A and C, from the pre-adult L4 stage, is sufficient to recapitulate the motility and longevity phenotypes of *daf-2(e1370)* mutants, which carry a single mutation in the DAF-2 kinase domain common to DAF-2A, C, D, and E isoforms (Kimura et al., 1997). Thus, DAF-2A and/or DAF-2C play a major role in the regulation of motility, lifespan, dauer, and oxidative stress resistance while the DAF-2D and E isoforms are not essential.

We detected DAF-2::AID::mNG receptor expression throughout the body, as in flies and mammals, and more extensively than previously appreciated using immunochemistry (Kimura et al., 2011). Interestingly, DAF-2::AID::mNG receptors fluorescence appeared as a punctate pattern in the cytoplasm of most cells, rather than enriched at the cell membrane. This pattern may highlight DAF-2/IIRc biosynthetic pathway and/or endosomal signaling compartment. Recent data obtained in mammalian cell culture also showed that the majority of insulin receptors are localized within intracellular vesicles under regular culture conditions (Boothe et al., 2016). Internalization of the insulin receptor is necessary to shut down insulin signaling, but it also induces endosome-specific signal transduction (Morcavallo et al., 2014). Increasing evidence suggests that alterations in the insulin receptor trafficking can lead to severe insulin resistance (Chen et al., 2019). *daf-2(kr462)* transgenic animals will be useful to further study the conservation of insulin/IGF-1 receptor biosynthesis and trafficking and its potential deregulation in the context of different *daf-2* mutants.

3.2 | DAF-2/IIRc activity in neurons and intestine limits wild-type lifespan via shared mechanisms that do not involve inter-organ inactivation of the DAF-2/IIRc

Our data pointed to the importance of both intestine and neurons for lifespan regulation by the DAF-2/IIRc pathway as reported in two recent studies using similar tools (Venz et al., 2021; Zhang et al., 2021). However, our results show some discrepancies with those of Zhang et al. who reported a lower extension of lifespan upon neuronal inactivation of DAF-2 (18%, as compared to 37 and 40% in our work and in Venz et al., respectively). Zhang et al. also observed a stronger impact of intestinal depletion of DAF-2 (which increased lifespan by 90%, as compared to 53% and 43% in our work and in Venz et al., respectively). This may be explained by a difference in the TIR1 strains used by Zhang et al., although we used different TIR1 strains to those of Venz et al. while obtaining similar results. Similarly, Uno et al. reported that down-regulation of DAF-2 by CRISPR or tissue-specific RNAi in the intestine or neurons extended worm lifespan by 40–60%. Overall, gut and neurons were the two tissues in which DAF-2 inactivation had the greatest impact on lifespan in all four studies, although hypodermis and germline may have a minor contribution (Uno et al., 2021; Zhang et al., 2021).

We further showed that combined DAF-2/IIRc degradation in the neurons and in the gut did not further extend the lifespan of the animals compared to worms with DAF-2/IIRc degradation in the gut. This suggests that DAF-2/IIRc signaling in the gut and neurons share

downstream mechanisms for the regulation of lifespan. Surprisingly, although intestinal DAF-2/IIRc inactivation conferred resistance of animals to oxidative stress, the correlation between longevity and oxidative stress resistance phenotypes was not verified with neuronal inactivation of DAF-2/IIRc. The link between oxidative stress resistance and lifespan extension has been a matter of intense debate for years (Dues et al., 2017, 2019). Our data suggest that while neuronal and intestinal DAF-2/IIRc affect lifespan through common mechanisms, those mechanisms do not seem to involve resistance to oxidative stress. However, we cannot exclude that our results might have been different if we had used another oxidative stressor, as we only studied a severe one (paraquat).

Shared mechanisms may result from the inactivation of DAF-2/IIRc in distant tissues (i.e., gut or neurons) when DAF-2/IIRc is inactivated in one tissue (i.e., neurons or gut, respectively) as previously proposed (Libina et al., 2003; Uno et al., 2021). However, our observations do not support this model, as neuronal or intestinal inactivation of DAF-2/IIRc triggered nuclear accumulation of DAF-16 in the same tissue, respectively (Figure 5). This discrepancy is probably linked to the lines used for monitoring DAF-16 subcellular localization. Previous studies used wild-type animals carrying an integrated multicopy array (*Pdaf-16::daf-16::gfp*) that exhibit several phenotypes that are reminiscent of DAF-16 gain-of-function (Henderson & Johnson, 2001). Therefore, gut and neuronal DAF-2/IIRc function in lifespan does not seem to depend on DAF-2/IIRc inactivation through inter-organ communication. *daf-2(e1370)* prevents loss of gut integrity (Gelino et al., 2016) and visceral pathologies associated with aging that limits worm survival (Ezcurra et al., 2018). During the last years, several longevity pathways have been shown to involve brain-gut communications in *C. elegans* (Berendzen et al., 2016; Durieux et al., 2011; Prahlad et al., 2008; Shao et al., 2016; Taylor & Dillin, 2013; Zhang et al., 2018), which may be explored using tissue-specific inactivation of DAF-2/IIRc to better understand the role of DAF-2/IIRc in lifespan regulation.

3.3 | Neuronal inactivation of DAF-2/IIRc downregulates motility in a DAF-16 dependent manner during early adulthood

Declined motility of worms with age has been associated with both decreased neuronal stimulation and the loss of muscle cell integrity (Liu et al., 2013; Mergoud Dit Lamarche et al., 2018; Mulcahy et al., 2013). Based on electrophysiological data, Liu et al. (2013) reported that synaptic transmission defects in motor neurons appear as early as day 5 of adulthood, while muscle contraction defects do not occur before day 11 of adulthood. They also showed that *daf-2(e1370)* mutation delayed the functional decline of neurons at the neuromuscular junction. Consistent with these data, we observed that whole-body inactivation of DAF-2 increased excitatory cholinergic neurotransmission at the neuromuscular junction in middle-aged animals, but also as early as day 1 of adulthood. (Figure S3). However, when we further tested DAF-2 inactivation in muscle or neurons only, worms did not show this phenotype at neither day 1 or day 14 of adulthood (Figure S2). Those data strongly suggest that the motility phenotype associated with *daf-2* inactivation in either muscle or neurons does not rely on the modulation of cholinergic transmission at the neuromuscular junction, although we cannot rule out subtle defects that would only be apparent at physiological concentrations of acetylcholine. Interestingly, those results also show that the increase in neurosecretion in *daf-2* mutants (our results and Liu et al., 2013) can be dissociated from their motility phenotype. The mechanisms responsible for this discrepancy remained to be elucidated.

3.4 | Muscle mitochondria morphology is regulated both autonomously and non-autonomously by DAF-2 activity

Mitochondria are dynamic organelles that undergo cycles of fusion and fission, important for the maintenance of their membrane potential and for mitophagy, respectively (Kleele et al., 2021). Interconnected or elongated mitochondria exhibit increased efficiency of ATP production and reduced generation of reactive oxygen species (ROS). Conversely, fragmented morphology is associated with reduced ATP production and uncoupling of mitochondria. Aberrant morphology and mitochondrial dysfunction are universal features of aging in invertebrates and vertebrates. In *C. elegans*, those changes may have a causal role in aging as modulation of either fusion or fission affect both lifespan and motility of worms (Byrne et al., 2019; Chaudhari & Kipreos, 2017; Liu et al., 2020; Weir et al., 2017). We and others have shown that muscle aging is associated with progressive mitochondria fragmentation (Mergoud Dit Lamarche et al., 2018; Regmi et al., 2014) that is delayed in *daf-2(e1370)* mutants (Mergoud Dit Lamarche et al., 2018).

Muscle inactivation of DAF-2/IIRc was sufficient to prevent fragmentation of mitochondria, suggesting that the increased motility of the worms relies on improved mitochondrial homeostasis. However, neuronal inactivation of DAF-2/IIRc protein resulted in a similar mitochondrial phenotype, but did not improve motility in middle age. Thus, although a young mitochondrial network may be a prerequisite for the maintenance of the neuromuscular system with aging, this may not be sufficient for the upregulation of motility by muscle DAF-2/IIRc.

3.5 | DAF-2 acts primarily in muscle to control motility in aging worms

Muscle DAF-2/IIRc plays a major role in the loss of worm motility observed in *daf-2* mutants, while it did not affect worm lifespan or resistance to oxidative stress. Furthermore, DAF-16/FOXO was dispensable for the regulation of motility by muscular DAF-2/IIRc while UNC-120/SRF was required. These observations agree with our

previous data obtained in the context of *daf-2(e1370)* mutants and support the cell-autonomous impact of DAF-2/UNC-120 on worm motility in middle age. Our results do not exclude the existence of a secondary signal from muscle to neurons that could improve motility. Indeed, previous work has identified the miRNA *mir-1*, as a regulator of a retrograde signal from muscle to neurons that modulates neuronal activity (Simon et al., 2008) and *mir-1* inactivation improves worm motility under pathological conditions (Schiffer et al., 2021). Interestingly, mammalian SRF has been shown to negatively regulate *mir-1* expression (Tritsch et al., 2013; Zhang et al., 2011). Identification of transcriptional targets of UNC-120/SRF in the context of muscle DAF-2 inactivation should help to better define the cellular mechanisms involved in the regulation of motility by muscle DAF-2.

Overall, we have developed and characterized a powerful tool to explore DAF-2 function with aging, uncovering unexpected findings regarding tissue-specific roles of DAF-2 in the regulation of dauer, lifespan, resistance to oxidative stress, and motility, as well as in the cross-talk between tissues.

Although both DAF-2 and DAF-16 are ubiquitously expressed, our approach identifies a tissue-specific, antagonistic, and age-dependent role for DAF-2/DAF-16 and DAF-2/UNC-120 signaling in the regulation of motility. Numerous phenotypes have been associated with *daf-2* mutants, and the future challenge will be to define the contribution of the different tissue-specific activities of DAF-2 in the regulation of these phenotypes and their downstream effectors.

4 | EXPERIMENTAL PROCEDURES

4.1 | *Caenorhabditis elegans* strains and media

All experiments were performed at 20°C except where specified. All strains were maintained at 20°C, except strain FS428 *daf-2(e1370)* III (corresponding to the original CB1370 strain outcrossed 6 times) which was maintained at 19°C to prevent larval arrest. Strains were grown on nematode growth medium (NGM) agar plates freshly poured and seeded with *Escherichia coli* OP50 culture. The wild-type reference strain was *C. elegans* N2 Bristol. All strains used in this study are described in Table S1.

4.2 | Plasmids and generation of single-copy insertion alleles

The plasmids constructed for this study are described in Table S5. Plasmids used to create single-copy insertion alleles by the mini-Mos method (Frøkjær-Jensen et al., 2014) are described in previous studies (Zhou et al., 2020, 2021), and the newly generated alleles are listed in Table S5. All constructs were verified by Sanger sequencing from GATC Company. For tissue-specific expression, the promoters used were as follows: *myo-3*– (body-wall muscle), *unc-47*– (GABAergic motoneuron), *unc-17*– (cholinergic motoneuron), *rab-3*– (pan-neuronal), *dpy-7*– (epidermis), or *eft-3*– (ubiquitous), N2 animals were injected with 15 ng/μL plasmid of interest containing the promoter and the open reading frame TIR1 or TOMM20 fused to fluorescent proteins, 50 ng/μL pCFJ601 (Mos1 transposase), 10 ng/μL pMA122 (negative selective marker *Phsp16.2::peel-1*), and 2.5 ng/μL pCFJ90 (*Pmyo-2::mCherry*). Neomycin (G418) was added to plates 24 h after injection at 1.5 μg/μL final concentration. Candidate plates were heat shocked for 2 h at 34°C. Selected lines were then bred to homozygosity and then crossed to generate the desired strains.

4.3 | Allele generation by CRISPR/Cas9 genome engineering

The generation of *kr462* and *kr535* alleles is described in Supplemental experimental procedures.

4.4 | Aging cohorts and auxin treatment

Auxin plates were prepared by adding auxin indole-3-acetic acid (Sigma-Aldrich) from a 400 mM stock solution in ethanol into NGM at the final concentration of 1 mM (Zhang et al., 2015). For control ethanol plates, the same volume of ethanol was added to NGM. Animals were transferred on auxin or ethanol plates at the L4 stage except for dauer tests for which eggs were laid and grown on auxin or ethanol plates.

For all aging cohorts, 20 μM 5-fluorouracil (5-FU, Sigma-Aldrich) was added to prevent progeny growth. Animals were transferred weekly to fresh plates, without 5-FU after 2 weeks. The day of transition to L4 is counted as day 0 of adulthood for the cohort.

4.5 | Dauer, lifespan and oxidative stress assays

Dauer, lifespan, and oxidative stress assays have been performed as described in Supplemental experimental procedures.

4.6 | Thrashing assays

For body bends frequency (BBF) measurements, 1-day-old or 13-day-old worms prepared as described in "aging cohorts" were gently transferred into a 12-well cell culture plate (ten worms per well) containing 1.5 mL of 2% agarose in M9 buffer (3 g KH_2PO_4, 6 g Na_2HPO_4, 5 g NaCl, 0.25 g $MgSO_4 \cdot 7\ H_2O$, and distilled water up to 1 L) and 2 mL of M9 buffer per well. Two minutes after transfer, animal movements were recorded for 30 s. BBF was then quantified using the open-source wrMTrck plugin on Fiji (ImageJ [v2.0.0]) software.

4.7 | Aldicarb assay

The tests were performed with synchronized worms. Twenty worms were added to a 100 μL drop of 250 μM aldicarb (Sigma,

ref. 33,386) in M9 buffer on polylysine-coated slides and incubated in a humidified chamber. 4, 4.5, 5, and 5.5 h later, the worms were stimulated with a blue light for 50 s and touched with a worm pick. With the blue light still on, their movement was then recorded for 30 s with the same device as for the thrashing tests. The recordings were made blind and the worms were considered paralyzed if they made less than three body bends during this recording.

Three biological replicates with independent cohorts were performed for each age.

4.8 | RNAi

RNAi feeding conditions are described in Supplemental experimental procedures.

4.9 | Microscopy and image processing

For all observations, animals were mounted on 2% agarose dry pads with 4% polystyrene beads (Polybeads, Polysciences) in M9 buffer. For images corresponding to Figures 1a, 2 and 5, and Figure S1, worms were observed using an Andor spinning disk system (Oxford Instruments) installed on a Nikon-IX86 microscope (Olympus) equipped with a 40x/NA 1.3 and a 60×/NA 1.42 oil-immersion objectives and an Evolve electron-multiplying charge-coupled device camera. Each animal was imaged with IQ software (APIS Informationstechnologien) as a stack of optical sections (0.3 µm apart) across the whole thickness of the worm (Figure 1a and Figure S1a) or across a specific tissue (Figures 2 and 4). All images were processed using the Fiji (ImageJ) software and correspond to the sums of the same number of slices (for each strain with or without auxin) except for images of the intestine (Figure 2g and Figure S1h) which correspond to z projection of maximum intensity. For fluorescence quantification, images covering the whole head including the most posterior pharyngeal bulb were summed (85 slices) and a ROI (180×230 pixels) was positioned relative to the middle of the most posterior part of the pharynx.

4.10 | Scoring of DAF-16 nuclear localization

One-day-old adults were observed using a AZ100 Multizoom Microscope (Nikon) equipped with a CMOS flash 4 C11440 (Hamammatsu) camera, for no more than 10 min per slide to avoid postmounting DAF-16::wrmSCARLET nuclear translocation. In absence of auxin, the fluorescence associated with DAF-16::wrmSCARLET appeared diffuse in the cytoplasm and nuclei of most tissues, except in the head neurons where it was completely excluded from the nuclei. A tissue was scored positive when several nuclei were brighter than the cytoplasm. Strains scoring and image analysis were performed blind.

4.11 | Scoring of muscle mitochondria morphology

Images of *krSi134*[*Pmyo-3::tomm-20N::wScarlet*] worms were acquired on an Axioscop compound microscope (Zeiss) equipped with a Neofluar 63x/NA 1.25 oil-immersion objective and a EMCC CoolSnap HQ (Photometrics) camera. For each worm, a representative image from the posterior body wall muscle cells was acquired. Cells with long interconnected mitochondrial networks were classified as interconnected; cells with a combination of interconnected mitochondrial networks along with some smaller fragmented mitochondria were classified as interrupted; cells with sparse small round mitochondria were classified as fragmented. Strains scoring and image analysis were performed blind.

4.12 | Statistical analysis

All statistical analyses were performed with R version 4.0.1 (2020-06-06). The R Test Survival Curve Differences (package survival_3.2–3) was used to analyze lifespan assays. This test is based on the *Grho* family of tests which makes use of the Kaplan–Meier estimate of survival (Fleming et al., 1982). Thrashing assays were analyzed using the non-parametric Kruskal–Wallis rank sum test, followed by Dunn's test of multiple comparisons (package rstatix_0.6.0) with FDR adjusting method as post hoc tests. To compare between different conditions for the mitochondria morphology assay, a Fisher exact test was performed, followed by pairwise tests with FDR adjusting method as post hoc tests (package rcompanion_2.4.1). For all tests, compared samples were considered different when statistical test gave an adjusted p-value <0.05 (*p <0.05; **p <0.01; ***p <0.001), ns: non-significant.

AUTHORS CONTRIBUTIONS

F.S and C.R. conceived the study. C.R., L.M., A.A., M.S., and F.S. performed the experiments. B.B. and C.V. constructed the mitochondria reporter strain and the TIR1 alleles, respectively. F.S. and C.R. analyzed and interpreted the data. The manuscript was written by F.S. and C.R. and edited by L.M. and J.-L.B.

ACKNOWLEDGEMENT

We thank the Caenorhabditis Genetic Center (which is funded by NIH Office of Research Infrastructure Programs, P40 OD010440) for strains. We are grateful to Laure Granger for technical assistance. This work was supported by the European Research Council (ERC_Adg C.NAPSE #695295), within the framework of the LABEX CORTEX (ANR-11-LABX-0042) of Université de Lyon and ANR-21-CE14-0026-01 operated by the French National Research Agency. CR was supported by a PhD fellowship from the French Ministry of Higher Education and Fondation de la recherche médicale (FDT202106012780). Biorender.com images were used to generate the graphical abstract within the framework of the LABEX CORTEX (ANR-11-LABX-0042) of Université de Lyon and

ANR-21-CE14-0026-01 operated by the French national research agency.

CONFLICT OF INTEREST

The authors declare no conflict of interest.

DATA AVAILABILITY STATEMENT

The authors confirm that the data supporting the findings of this study are available within the article and its supplementary materials. The strains generated in this study will be shared by the lead contact upon request.

ORCID

Florence Solari https://orcid.org/0000-0002-4173-8314

REFERENCES

Aghayeva, U., Bhattacharya, A., Sural, S., Jaeger, E., Churgin, M., Fang-Yen, C., & Hobert, O. (2021). DAF-16/FoxO and DAF-12/VDR control cellular plasticity both cell-autonomously and via interorgan signaling. *PLoS Biology*, *19*, e3001204. https://doi.org/10.1371/journal.pbio.3001204

Bansal, A., Zhu, L. J., Yen, K., & Tissenbaum, H. A. (2015). Uncoupling lifespan and healthspan in *Caenorhabditis elegans* longevity mutants. *Proceedings of the National Academy of Sciences of the United States of America*, *112*, E277–E286. https://doi.org/10.1073/pnas.1412192112

Berendzen, K. M., Durieux, J., Shao, L. W., Tian, Y., Kim, H. E., Wolff, S., Liu, Y., & Dillin, A. (2016). Neuroendocrine coordination of mitochondrial stress signaling and proteostasis. *Cell*, *166*, 1553-1563. e10. https://doi.org/10.1016/j.cell.2016.08.042

Bhattacharya, A., Aghayeva, U., Berghoff, E. G., & Hobert, O. (2019). Plasticity of the electrical connectome of *C. elegans*. *Cell*, *176*, 1174-1189.e16. https://doi.org/10.1016/j.cell.2018.12.024

Boothe, T., Lim, G. E., Cen, H., Skovsø, S., Piske, M., Li, S. N., Nabi, I. R., Gilon, P., & Johnson, J. D. (2016). Inter-domain tagging implicates caveolin-1 in insulin receptor trafficking and Erk signaling bias in pancreatic beta-cells. *Molecular Metabolism*, *5*, 366–378. https://doi.org/10.1016/j.molmet.2016.01.009

Byrne, J. J., Soh, M. S., Chandhok, G., Vijayaraghavan, T., Teoh, J. S., Crawford, S., Cobham, A. E., Yapa, N. M. B., Mirth, C. K., & Neumann, B. (2019). Disruption of mitochondrial dynamics affects behaviour and lifespan in *Caenorhabditis elegans*. *Cellular and Molecular Life Sciences: CMLS*, *76*, 1967–1985. https://doi.org/10.1007/s00018-019-03024-5

Chaudhari, S. N., & Kipreos, E. T. (2017). Increased mitochondrial fusion allows the survival of older animals in diverse *C. elegans* longevity pathways. *Nature Communications*, *8*, 182. https://doi.org/10.1038/s41467-01700274-4

Chen, Y., Huang, L., Qi, X., & Chen, C. (2019). Insulin receptor trafficking: consequences for insulin sensitivity and diabetes. *International Journal of Molecular Sciences*, *20*, E5007. https://doi.org/10.3390/ijms20205007

Churgin, M. A., Jung, S.-K., Yu, C.-C., Chen, X., Raizen, D. M., & Fang-Yen, C. (2017). Longitudinal imaging of *Caenorhabditis elegans* in a microfabricated device reveals variation in behavioral decline during aging. *eLife*, *6*, e26652. https://doi.org/10.7554/eLife.26652

Dillin, A., Crawford, D. K., & Kenyon, C. (2002). Timing requirements for insulin/IGF-1 signaling in *C. elegans*. *Science*, *298*, 831–834. https://doi.org/10.1126/science.1074240

Dues, D. J., Andrews, E. K., Senchuk, M. M., & Van Raamsdonk, J. M. (2019). Resistance to stress can be experimentally dissociated from longevity. *The Journals of Gerontology. Series A, Biological Sciences and Medical Sciences*, *74*, 1206–1214. https://doi.org/10.1093/gerona/gly213

Dues, D. J., Schaar, C. E., Johnson, B. K., Bowman, M. J., Winn, M. E., Senchuk, M. M., & van Raamsdonk, J. M. (2017). Uncoupling of oxidative stress resistance and lifespan in long-lived isp-1 mitochondrial mutants in *Caenorhabditis elegans*. *Free Radical Biology & Medicine*, *108*, 362–373. https://doi.org/10.1016/j.freeradbiomed.2017.04.004

Duhon, S. A., & Johnson, T. E. (1995). Movement as an index of vitality: Comparing wild type and the age-1 mutant of *Caenorhabditis elegans*. *The Journals of Gerontology. Series A, Biological Sciences and Medical Sciences*, *50*, B254–B261. https://doi.org/10.1093/geronа/50a.5.b254

Durieux, J., Wolff, S., & Dillin, A. (2011). The cell-non-autonomous nature of electron transport chainmediated longevity. *Cell*, *144*, 79–91. https://doi.org/10.1016/j.cell.2010.12.016

Ezcurra, M., Benedetto, A., Sornda, T., Gilliat, A. F., Au, C., Zhang, Q., van Schelt, S., Petrache, A. L., Wang, H., de la Guardia, Y., Bar-Nun, S., Tyler, E., Wakelam, M. J., & Gems, D. (2018). *C. elegans* eats its own intestine to make yolk leading to multiple senescent pathologies. *Current Biology: CB*, *28*, 2544–2556.e5. https://doi.org/10.1016/j.cub.2018.06.035

Fleming, T. R., Green, S. J., & Harrington, D. P. (1982). Performing serial testing of treatment effects. *Experientia. Supplementum*, *41*, 469–484.

Frøkjær-Jensen, C., Davis, M. W., Sarov, M., Taylor, J., Flibotte, S., LaBella, M., Pozniakovsky, A., Moerman, D. G., & Jorgensen, E. M. (2014). Random and targeted transgene insertion in *Caenorhabditis elegans* using a modified Mos 1 transposon. *Nature Methods*, *11*, 529–534. https://doi.org/10.1038/nmeth.2889

Gelino, S., Chang, J. T., Kumsta, C., She, X., Davis, A., Nguyen, C., Panowski, S., & Hansen, M. (2016). Intestinal autophagy improves healthspan and longevity in *C. elegans* during dietary restriction. *PLoS Genetics*, *12*, e1006135. https://doi.org/10.1371/journal.pgen.1006135

Gems, D., Sutton, A. J., Sundermeyer, M. L., Albert, P. S., King, K. V., Edgley, M. L., Larsen, P. L., & Riddle, D. L. (1998). Two pleiotropic classes of daf-2 mutation affect larval arrest, adult behavior, reproduction and longevity in *Caenorhabditis elegans*. *Genetics*, *150*, 129–155. https://doi.org/10.1093/genetics/150.1.129

Hahm, J.-H., Kim, S., DiLoreto, R., Shi, C., Lee, S. J., Murphy, C. T., & Nam, H. G. (2015). *C. elegans* maximum velocity correlates with healthspan and is maintained in worms with an insulin receptor mutation. *Nature Communications*, *6*, 8919. https://doi.org/10.1038/ncomms9919

Henderson, S. T., & Johnson, T. E. (2001). daf-16 integrates developmental and environmental inputs to mediate aging in the nematode *Caenorhabditis elegans*. *Current Biology: CB*, *11*, 1975–1980. https://doi.org/10.1016/s0960-9822(01)00594-2

Honda, Y., & Honda, S. (2002). Oxidative stress and life span determination in the nematode *Caenorhabditis elegans*. *Annals of the New York Academy of Sciences*, *959*, 466–474. https://doi.org/10.1111/j.1749632.2002.tb02117.x

Hsu, A.-L., Feng, Z., Hsieh, M.-Y., & Xu, X. Z. S. (2009). Identification by machine vision of the rate of motor activity decline as a lifespan predictor in *C. elegans*. *Neurobiology of Aging*, *30*, 1498–1503. https://doi.org/10.1016/j.neurobiolaging.2007.12.007

Huang, C., Xiong, C., & Kornfeld, K. (2004). Measurements of age-related changes of physiological processes that predict lifespan of *Caenorhabditis elegans*. *Proceedings of the National Academy of Sciences of the United States of America*, *101*, 8084–8089. https://doi.org/10.1073/pnas.0400848101

Kenyon, C., Chang, J., Gensch, E., Rudner, A., & Tabtiang, R. (1993). A *C. elegans* mutant that lives twice as long as wild type. *Nature*, *366*, 461–464. https://doi.org/10.1038/366461a0

Kenyon, C. J. (2010). The genetics of ageing. *Nature*, *464*, 504–512. https://doi.org/10.1038/nature08980

Kimura, K. D., Riddle, D. L., & Ruvkun, G. (2011). The *C. elegans* DAF-2 insulin-like receptor is abundantly expressed in the nervous system and regulated by nutritional status. *Cold Spring Harbor Symposia on Quantitative Biology*, *76*, 113–120. https://doi.org/10.1101/sqb.2011.76.010660

Kimura, K. D., Tissenbaum, H. A., Liu, Y., & Ruvkun, G. (1997). daf-2, an insulin receptor-like gene that regulates longevity and diapause in *Caenorhabditis elegans*. *Science*, *277*, 942–946. https://doi.org/10.1126/science.277.5328.942

Kleele, T., Rey, T., Winter, J., Zaganelli, S., Mahecic, D., Perreten Lambert, H., Ruberto, F. P., Nemir, M., Wai, T., Pedrazzini, T., & Manley, S. (2021). Distinct fission signatures predict mitochondrial degradation or biogenesis. *Nature*, *593*, 435–439. https://doi.org/10.1038/s41586-021-03510-6

Laranjeiro, R., Harinath, G., Hewitt, J. E., Hartman, J. H., Royal, M. A., Meyer, J. N., Vanapalli, S. A., & Driscoll, M. (2019). Swim exercise in *Caenorhabditis elegans* extends neuromuscular and gut healthspan, enhances learning ability, and protects against neurodegeneration. *Proceedings of the National Academy of Sciences of the United States of America*, *116*, 23829. https://doi.org/10.1073/pnas.1909210116

Lee, R. Y., Hench, J., & Ruvkun, G. (2001). Regulation of *C. elegans* DAF-16 and its human ortholog FKHRL1 by the daf-2 insulin-like signaling pathway. *Current Biology: CB*, *11*, 1950–1957. https://doi.org/10.1016/s09609822(01)00595-4

Li, W.-J., Wang, C.-W., Tao, L., Yan, Y. H., Zhang, M. J., Liu, Z. X., Li, Y. X., Zhao, H. Q., Li, X. M., He, X. D., Xue, Y., & Dong, M. Q. (2021). Insulin signaling regulates longevity through protein phosphorylation in *Caenorhabditis elegans*. *Nature Communications*, *12*, 4568. https://doi.org/10.1038/s41467021-24816-z

Libina, N., Berman, J. R., & Kenyon, C. (2003). Tissue-specific activities of *C. elegans* DAF-16 in the regulation of lifespan. *Cell*, *115*, 489–502. https://doi.org/10.1016/S0092-8674(03)00889-4

Lin, K., Dorman, J. B., Rodan, A., & Kenyon, C. (1997). daf-16: An HNF-3/forkhead family member that can function to double the life-span of *Caenorhabditis elegans*. *Science*, *278*, 1319–1322. https://doi.org/10.1126/science.278.5341.1319

Lin, K., Hsin, H., Libina, N., & Kenyon, C. (2001). Regulation of the *Caenorhabditis elegans* longevity protein DAF-16 by insulin/IGF-1 and germline signaling. *Nature Genetics*, *28*, 139–145. https://doi.org/10.1038/88850

Liu, J., Zhang, B., Lei, H., Feng, Z., Liu, J., Hsu, A. L., & Xu, X. Z. S. (2013). Functional aging in the nervous system contributes to age dependent motor activity decline in *C. elegans*. *Cell Metabolism*, *18*, 392–402. https://doi.org/10.1016/j.cmet.2013.08.007

Liu, Y. J., McIntyre, R. L., Janssens, G. E., Williams, E. G., Lan, J., van Weeghel M., Schomakers B., van der Veen H., van der Wel, N. N., Yao, P., Mair, W. B., Aebersold, R., MacInnes, A. W., & Houtkooper, R. H. (2020). Mitochondrial translation and dynamics synergistically extend lifespan in *C. elegans* through HLH-30. *The Journal of Cell Biology*, *219*, e201907067. https://doi.org/10.1083/jcb.201907067

Martinez, B. A., Reis Rodrigues, P., Nuñez Medina, R. M., Mondal, P., Harrison, N. J., Lone, M. A., Webster, A., Gurkar, A. U., Grill, B., & Gill, M. S. (2020). An alternatively spliced, non-signaling insulin receptor modulates insulin sensitivity via insulin peptide sequestration in *C. elegans*. *eLife*, *9*, e49917. https://doi.org/10.7554/eLife.49917

Mergoud Dit Lamarche, A., Molin, L., Pierson, L., Mariol, M. C., Bessereau, J. L., Gieseler, K., & Solari, F. (2018). UNC-120/SRF independently controls muscle aging and lifespan in *Caenorhabditis elegans*. *Aging Cell*, *17*, e12713. https://doi.org/10.1111/acel.12713

Morcavallo, A., Stefanello, M., Iozzo, R. V., Belfiore, A., & Morrione, A. (2014). Ligand-mediated endocytosis and trafficking of the insulin-like growth factor receptor I and insulin receptor modulate receptor function. *Frontiers in Endocrinology*, *5*, 220. https://doi.org/10.3389/fendo.2014.00220

Mulcahy, B., Holden-Dye, L., & O'Connor, V. (2013). Pharmacological assays reveal age-related changes in synaptic transmission at the *Caenorhabditis elegans* neuromuscular junction that are modified by reduced insulin signalling. *The Journal of Experimental Biology*, *216*(3), 492–501. https://doi.org/10.1242/jeb.068734

Ogg, S., Paradis, S., Gottlieb, S., Patterson, G. I., Lee, L., Tissenbaum, H. A., & Ruvkun, G. (1997). The Fork head transcription factor DAF-16 transduces insulinlike metabolic and longevity signals in *C. elegans*. *Nature*, *389*, 994–999. https://doi.org/10.1038/40194

Ohno, H., Kato, S., Naito, Y., Kunitomo, H., Tomioka, M., & Iino, Y. (2014). Role of synaptic phosphatidylinositol 3-kinase in a behavioral learning response in *C. elegans*. *Science*, *345*, 313–317. https://doi.org/10.1126/science.1250709

Podshivalova, K., Kerr, R. A., & Kenyon, C. (2017). How a mutation that slows aging can also disproportionately extend end-of-life decrepitude. *Cell Reports*, *19*, 441–450. https://doi.org/10.1016/j.celrep.2017.03.062

Prahlad, V., Cornelius, T., & Morimoto, R. I. (2008). Regulation of the cellular heat shock response in *Caenorhabditis elegans* by thermosensory neurons. *Science*, *320*, 811–814. https://doi.org/10.1126/science.1156093

Regmi, S. G., Rolland, S. G., & Conradt, B. (2014). Age-dependent changes in mitochondrial morphology and volume are not predictors of lifespan. *Aging*, *6*, 118–130. https://doi.org/10.18632/aging.100639

Schiffer, I., Gerisch, B., Kawamura, K., Laboy, R., Hewitt, J., Denzel, M. S., Mori, M. A., Vanapalli, S., Shen, Y., Symmons, O., & Antebi, A. (2021). miR-1 coordinately regulates lysosomal v-ATPase and biogenesis to impact proteotoxicity and muscle function during aging. *eLife*, *10*, e66768. https://doi.org/10.7554/eLife.66768

Shao, L.-W., Niu, R., & Liu, Y. (2016). Neuropeptide signals cell non-autonomous mitochondrial unfolded protein response. *Cell Research*, *26*, 1182–1196. https://doi.org/10.1038/cr.2016.118

Sharma, A., Smith, H. J., Yao, P., & Mair, W. B. (2019). Causal roles of mitochondrial dynamics in longevity and healthy aging. *EMBO Reports*, *20*, e48395. https://doi.org/10.15252/embr.201948395

Simon, D. J., Madison, J. M., Conery, A. L., Thompson-Peer, K. L., Soskis, M., Ruvkun, G. B., Kaplan, J. M., & Kim, J. K. (2008). The microRNA miR-1 regulates a MEF-2-dependent retrograde signal at neuromuscular junctions. *Cell*, *133*, 903–915. https://doi.org/10.1016/j.cell.2008.04.035

Taylor, R. C., & Dillin, A. (2013). XBP-1 is a cell-nonautonomous regulator of stress resistance and longevity. *Cell*, *153*, 1435–1447. https://doi.org/10.1016/j.cell.2013.05.042

Taylor, S. R., Santpere, G., Weinreb, A., Barrett, A., Reilly, M. B., Xu, C., Varol, E., Oikonomou, P., Glenwinkel, L., McWhirter, R., Poff, A., Basavaraju, M., Rafi, I., Yemini, E., Cook, S. J., Abrams, A., Vidal, B., Cros, C., Tavazoie, S., … Miller 3rd, D. M.. (2021). Molecular topography of an entire nervous system. *Cell*, *184*, 4329–4347.e23. https://doi.org/10.1016/j.cell.2021.06.023

Tepper, R. G., Ashraf, J., Kaletsky, R., Kleemann, G., Murphy, C. T., & Bussemaker, H. J. (2013). PQM-1 complements DAF-16 as a key transcriptional regulator of DAF-2-mediated development and longevity. *Cell*, *154*, 676–690. https://doi.org/10.1016/j.cell.2013.07.006

Tritsch, E., Mallat, Y., Lefebvre, F., Diguet, N., Escoubet, B., Blanc, J., de Windt, L. J., Catalucci, D., Vandecasteele, G., Li, Z., & Mericskay, M. (2013). An SRF/miR-1 axis regulates NCX1 and annexin A5 protein levels in the normal and failing heart. *Cardiovascular Research*, *98*, 372–380. https://doi.org/10.1093/cvr/cvt042

Uno, M., Tani, Y., Nono, M., Okabe, E., Kishimoto, S., Takahashi, C., Abe, R., Kurihara, T., & Nishida, E. (2021). Neuronal DAF-16-to-intestinal

DAF-16 communication underlies organismal lifespan extension in *C. elegans*. *iScience*, *24*, 102706. https://doi.org/10.1016/j.isci.2021.102706

Venz, R., Pekec, T., Katic, I., Ciosk, R., & Ewald, C. Y. (2021). End-of-life targeted degradation of DAF-2 insulin/IGF-1 receptor promotes longevity free from growth-related pathologies. *eLife*, *10*, e71335. https://doi.org/10.7554/eLife.71335

Weir, H. J., Yao, P., Huynh, F. K., Escoubas, C. C., Goncalves, R. L., Burkewitz, K., Laboy, R., Hirschey, M. D., & Mair, W. B. (2017). Dietary restriction and AMPK increase lifespan via mitochondrial network and peroxisome remodeling. *Cell Metab*, *26*, 884–896.e5. https://doi.org/10.1016/j.cmet.2017.09.024

Wolkow, C. A., Kimura, K. D., Lee, M.-S., & Ruvkun, G. (2000). Regulation of C. elegans life-span by insulinlike signaling in the nervous system. *Science*, *290*, 5.

Zhang, B., Gong, J., Zhang, W., Xiao, R., Liu, J., & Xu, X. Z. S. (2018). Brain-gut communications via distinct neuroendocrine signals bidirectionally regulate longevity in *C. elegans*. *Genes & Development*, *32*, 258–270. https://doi.org/10.1101/gad.309625.117

Zhang, L., Ward, J. D., Cheng, Z., & Dernburg, A. F. (2015). The auxin-inducible degradation (AID) system enables versatile conditional protein depletion in *C. elegans*. *Development*, *142*, 4374–4384. https://doi.org/10.1242/dev.129635

Zhang, X., Azhar, G., Helms, S. A., & Wei, J. Y. (2011). Regulation of cardiac microRNAs by serum response factor. *Journal of Biomedical Science*, *18*, 15. https://doi.org/10.1186/1423-0127-18-15

Zhang, Y.-P., Zhang, W.-H., Zhang, P., Li, Q., Sun, Y., Wang, J.-W., Zhang, S.-B. O., Cai, T., Zhan, C., & Dong, M.-Q. (2021). Degrading intestinal DAF-2 nearly doubles *Caenorhabditis elegans* lifespan without affecting development or reproduction. *bioRxiv*. http://biorxiv.org/lookup/doi/10.1101/2021.07.31.454567

Zhen, M., & Samuel, A. D. T. (2015). *C. elegans* locomotion: Small circuits, complex functions. *Current Opinion in Neurobiology*, *33*, 117–126. https://doi.org/10.1016/j.conb.2015.03.009

Zhou, X., Gueydan, M., Jospin, M., Ji, T., Valfort, A., Pinan-Lucarré, B., & Bessereau, J. L. (2020). The netrin receptor UNC-40/DCC assembles a postsynaptic scaffold and sets the synaptic content of GABAA receptors. *Nature Communications*, *11*, 2674. https://doi.org/10.1038/s41467-020-16473-5

Zhou, X., Vachon, C., Cizeron, M., Romatif, O., Bülow, H. E., Jospin, M., & Bessereau, J. L. (2021). The HSPG syndecan is a core organizer of cholinergic synapses. *The Journal of Cell Biology*, *220*, e202011144. https://doi.org/10.1083/jcb.202011144

SUPPORTING INFORMATION

Additional supporting information can be found online in the Supporting Information section at the end of this article.

How to cite this article: Roy, C., Molin, L., Alcolei, A., Solyga, M., Bonneau, B., Vachon, C., Bessereau, J-L, & Solari, F. (2022). DAF-2/insulin IGF-1 receptor regulates motility during aging by integrating opposite signaling from muscle and neuronal tissues. *Aging Cell*, *21*, e13660. https://doi.org/10.1111/acel.13660